Anisotropic path and site effects' influences on strong ground motion records in the Santa Barbara region.

Ken Hudson, PhD, PG, EIT[1]

[1]Hudson Geotechnics, Inc. (ken@hudsongeotechnics.com)

June 30, 2025

Introduction

Santa Barbara, California, lies in a seismically active region, where the complex interplay of faults generates significant earthquake hazards. Understanding ground motions— the shaking intensity caused by earthquakes— is critical for designing resilient infrastructure. The National Seismic Hazard Model (NSHM), developed by the U.S. Geological Survey, provides the basis for building code design ground motions. In Santa Barbara, these design ground motions are notably high due to the region's proximity to local faults (**Figure 1**). With each updated edition of the NSHM, advancements in seismic hazard modeling, including refined fault characterizations and improved ground motion models, have led to progressively higher design ground motion (**Figure 2**).

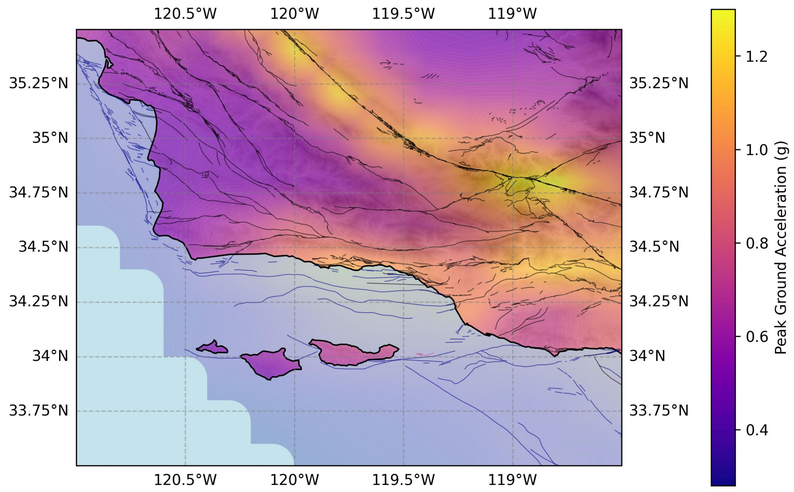

Figure 1: NSHM23 (Petersen et al. 2023) Site Class D Probabilistic Seismic Hazard PGA for 2% probability of exceedance in 50 years (2,475-year return period)

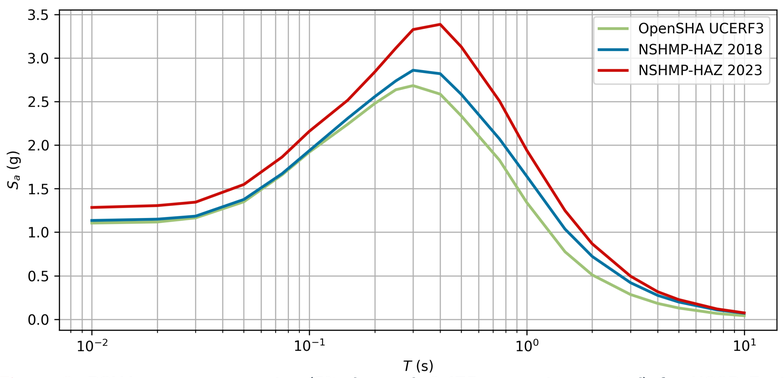

Figure 2: PSHA response spectra (5% damped, 2,475-year return period) for UCSB East Campus using different earthquake rupture forecasts

Several recording stations exist in the Santa Barbara region, in particular this study focuses on CI.USB, a downhole strong motion station located on UCSB's campus next to Webb Hall (**Figure 3**).

CI.USB has V_{S30}~300 m/s; the subsurface is characterized by shallow terrace deposits (~10ft thick) overlying Sisquoc formation siltstone

Figure 3: CI.USB during ARRA project site characterization (Yong et al. 2013).

Dataset and Analysis

ObsPy (Beyreuther et al. 2010) and gmprocess are used to identify events in the region from 2011 to the present and download/process records, respectively. 489 records are successfully downloaded and processed (**Figure 4**).

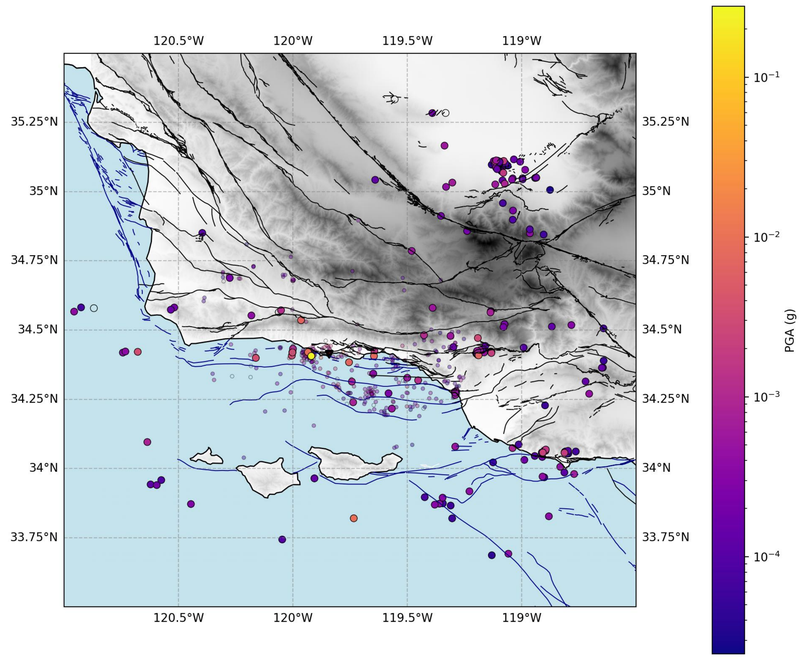

Figure 4: Earthquake epicenters from 2011 to the present and the PGA recorded at CI.USB.

A GMM (Boore et al. 2014) is used to predict IMs, and residuals ($R_{i,j}$) with respect to recorded IMs are computed at CI.USB (**Figures 5 & 6**). Of particular note is the 2013 M4.8 that occurred approximately 7km west of CI.USB and caused significant PGA at the station.

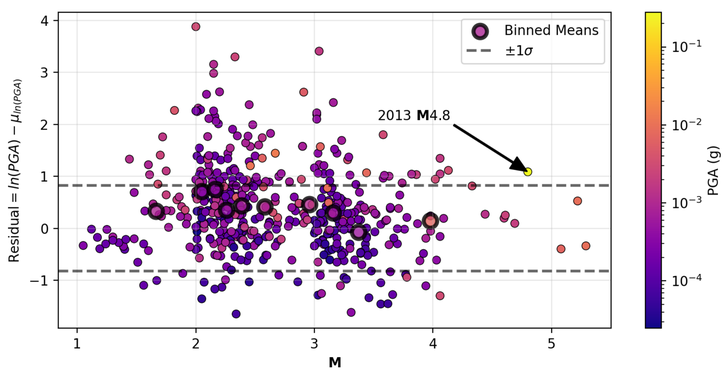

Figure 5: Residuals of PGA against earthquake magnitude at CI.USB.

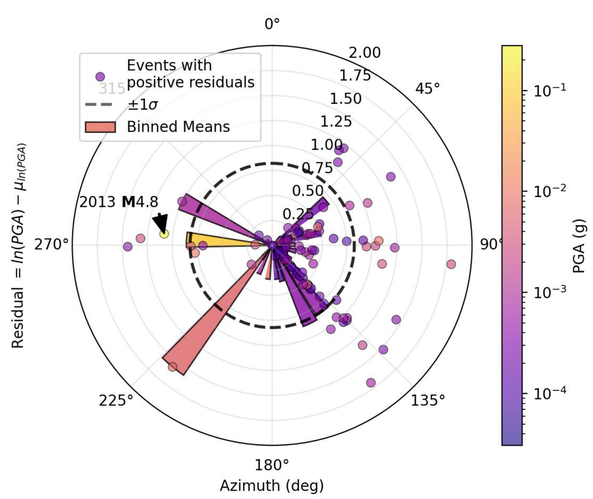

Figure 6: Residuals of PGA against azimuth (for M>=3) at CI.USB.

To examine the 2013 **M**4.8 event, gmprocess (Thompson et al. 2024) is used to process 228 records (**Figure 7**) from the event and a large number of records from several dozen events in the region. A mixed-effects regression is performed to examine the event term (η_i) and within event residual ($\delta W_{i,j}$):

$$R_{i,j} = c_0 + \eta_i + \delta W_{i,j}$$

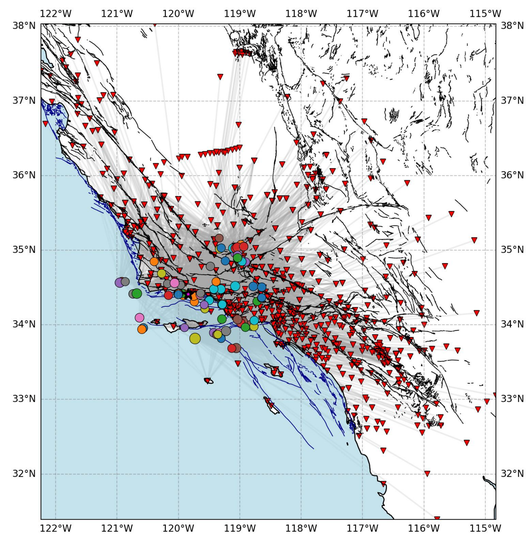

Figure 7: Stations and earthquakes with recordings used for mixed-effects regression of residuals.

The sum of the total bias and event term for the 2013 **M**4.8 is found to be -0.86, meaning that on average the event is **overpredicted** and the recording at CI.USB is shown to be a significantly larger PGA than expected for this event (**Figure 8**).

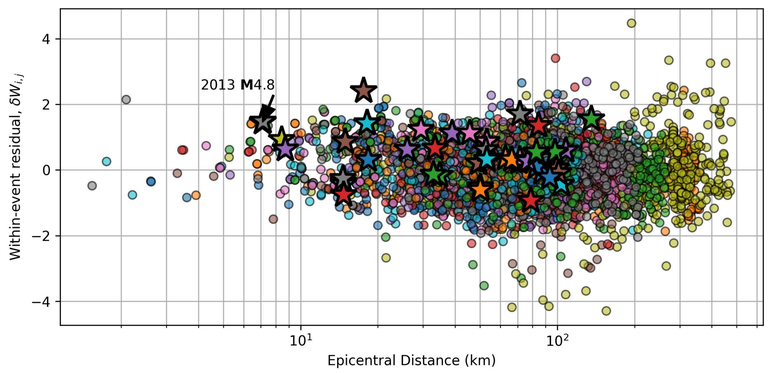

Figure 8: Within-event residuals with epicentral distance (colors indicate earthquake)

Earthquake Horizontal-to-Vertical Spectral Ratios (eHVSR) are computed for the 489 records at CI.USB to explore azimuthal dependence (**Figure 9**).

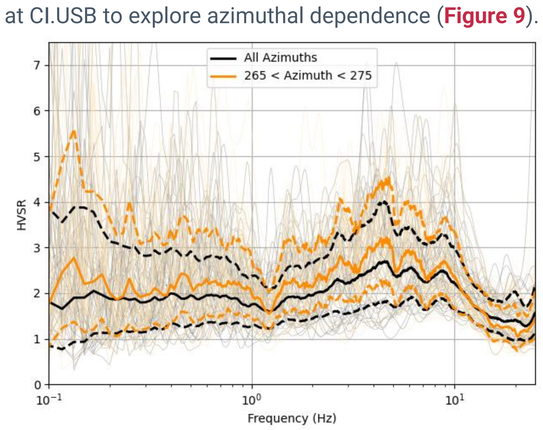

Figure 9: eHVSR at CI.USB.

Petersen, M. D., A. M. Shumway, P. M. Powers, N. Field, Moschetti, K. Jaiswal, K. R. Milner, S. Rezaeian, A. D. Frankel, A. L. Llenos, A. J. Michael, J. M. Altekruse, S. K. Ahdi, K. Withers, C. S. Mueller, Y. Zeng, R. E. Chase, L. M. Salditch, N. Luco, K. S. Rukstales, J. A. Herrick, D. L. Girot, B. T. Aagaard, A. M. Bender, M. L. Blanpied, R. Briggs, O. S. Boyd, B. S. Clayton, C. B. Duross, E. Evans, P. J. Haeussler, A. E. Alexandra E Hatem, K. L. Haynie, E. Hearn, K. Johnson, Z. A. Kortum, N. (Simon) Kwong, A. J. Makdisi, H. (Ben) B. Mason, D. E. McNamara, D. F. McPhillips, P. G. Okubo, M. T. Page, F. Pollitz, J. L. Rubinstein, B. Shaw, Z.-K. Shen, B. R. Shiro, J. A. Smith, W. J. Stephenson, E. M. Thompson, J. A. Jobe, E. (Wirth) W. Moriarty, and R. C. Witter. 2023. "Data Release for the 2023 U.S. 50-State National Seismic Hazard Model - Overview." U.S. Geological Survey.

Yong, A., A. Martin, K. Stokoe, and J. Diehl. 2013. *ARRA-Funded VS30 Measurements Using Multi-Technique Approach at Strong-Motion Stations in California and Central-Eastern United States*. U.S. Geological Survey Open-File Report.

Boore, D. M., J. P. Stewart, E. Seyhan, and G. M. Atkinson. 2014. "NGA-West2 Equations for Predicting PGA, PGV, and 5% Damped PSA for Shallow Crustal Earthquakes." *Earthquake Spectra*, 30 (3): 1057–1085. https://doi.org/10.1193/070113EQS184M.

Thompson, E. M., M. Hearne, B. T. Aagaard, J. M. Rekoske, Worden, M. P. Moschetti, H. E. Hunsinger, G. C. Ferragut, G. A. Parker, J. A. Smith, K. K. Smith, and A. R. Kottke. 2024. "USGS Automated Ground Motion Processing Software version 2." U.S. Geological Survey.